Development of Complex Classical Force Fields through Force Matching to ab Initio Data: Application to a Room-Temperature Ionic Liquid

Tristan G. A. Youngs,* Mario G. Del Pópolo, and Jorge Kohanoff

Atomistic Simulation Centre, School of Physics, Queen's University, Belfast BT7 1NN, United Kingdom

Received: November 29, 2005; In Final Form: January 25, 2006

Recent experimental neutron diffraction data and ab initio molecular dynamics simulation of the ionic liquid dimethylimidazolium chloride ([dmim]Cl) have provided a structural description of the system at the molecular level. However, partial radial distribution functions calculated from the latter, when compared to previous classical simulation results, highlight some limitations in the structural description offered by force field-based simulations. With the availability of ab initio data it is possible to improve the classical description of [dmim]Cl by using the force matching approach, and the strategy for fitting complex force fields in their original functional form is discussed. A self-consistent optimization method for the generation of classical potentials of general functional form is presented and applied, and a force field that better reproduces the observed first principles forces is obtained. When used in simulation, it predicts structural data which reproduces more faithfully that observed in the ab initio studies. Some possible refinements to the technique, its application, and the general suitability of common potential energy functions used within many ionic liquid force fields are discussed.

Introduction

Ionic liquids (ILs) are receiving much attention of late owing to their potential application in many areas of chemistry. They are molecular fluids composed usually of large organic cations and inorganic anions, have melting points close to or below ambient temperature, and show negligible vapor pressure.[1,2] In many cases they have been shown to enhance chemical reactivity and selectivity,[3,4] and coupled with their recoverability this has led to them being considered "green" solvents for use in organic synthesis. However, since the liquid phase is less tractable by experimental investigation, their unique properties are not yet fully understood despite the significant volume of work geared toward assessing potential applications.

One of the most common families of ILs consists of dialkylimidazolium cations coupled with inorganic anions such as chloride, tetrafluoroborate, or hexafluorophosphate. The focus of this paper, 1,3-dimethylimidazolium chloride ([dmim]Cl, Figure 1), is one of the simplest imidazolium-based IL and is a valuable target for study owing to its position as a "model" system. Its simplicity has led to it being one of the few ILs so far investigated by neutron diffraction, such experiments performed by Hardacre et al.[5] providing valuable data on the liquid structure. In addition, the variation of liquid density as a function of temperature has been described by Fannin et al.[6] For imidazolium-based ILs other than [dmim]Cl, numerous synthetic applications have been investigated[3,4,7] and a wide range of properties have been examined, experiments providing, for example, polarities,[8] activity coefficients of various types of molecule,[9] viscosities, compressibilities, and speed of sound measurements.[10−12]

Theoretical studies centered on classical simulation have proven to be useful complements to experiment, offering the possibility of studying interactions in systems at the atomic level.

* Address correspondence to this author. Phone: +44 (2890) 973528. Fax: +44 (2890) 975359. E-mail: t.youngs@qub.ac.uk.

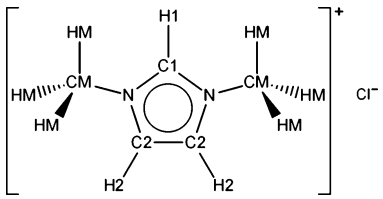

Figure 1. Structure and atomic labeling of dimethylimidazolium chloride ([dmim]Cl).

Molecular dynamics (MD) and Monte Carlo (MC) methods have been used in studies of many ILs to calculate, for example, gas solubilities,[13,14] solvation free energies of small molecules,[15] properties of aqueous mixtures,[16,17] liquid−liquid and liquid−vapor interfaces,[18,19] metal ion complexation,[20,21] and the structure and dynamics of ILs under confinement.[22] Given the reliance on simulation in furthering our knowledge of these systems, the need for accurate models is clear.

Existing Force Fields

Force fields for the MD and MC simulation of ionic liquids consist generally of pairwise short-range repulsive−dispersive potentials of the Lennard-Jones (LJ) or Buckingham type, with long-range electrostatics modeled by using atomic point charges and bonded interactions represented by simple harmonic (bond and angle) and cosine (torsional) potentials. Commonly, point charges and cation geometry are calculated by ab initio means at the author's discretion, while short-range parameters and relevant geometric force constants are taken from established sources such as OPLS,[23] AMBER,[24] or CHARMM.[25] As these force fields have been designed for the simulation of proteins, and since the protonated histidine (His+) residue is 1,3-dihydroimidazolium, many (but not all) parameters relevant to the alkylimidazolium family of ILs are readily available. However, the transferability of parameters from these force fields (developed primarily with the simulation of biological/

10.1021/jp056931k CCC: $33.50
Published on Web 03/02/2006

TABLE 1: Main Properties of Published [dmim]Cl Forcefields

model	type[a]	VDW	charges[b]	geometry[c]
CLDP	AA	LJ (OPLS)	CHELPG[27]	RHF/6-31G*
			MP2/cc-pVTZ(-f)	OPLS/AMBER
UR	UA	LJ (OPLS)	Mulliken	B3LYP/6-311+G*
			MP2/6-311G*	CHARM22
HPLB	AA[d]	Buckingham[28−30]	DMA[31]	RHF/6-31G**
			MP2/6-31G**	(rigid cation)
LHW	AA	LJ (AMBER)	RESP[32]	RHF/6-31+G*
			RHF/6-31+G*	AMBER

[a] Denotes explicit hydrogen (all-atom, AA) or implicit hydrogen (united-atom, UA) formalism. [b] Method of charge derivation (CHELPG = charges from electrostatic potential grid method, Mulliken = charges derived from Mulliken population analysis, DMA = distributed multipole analysis, RESP = restricted electrostatic potential method) and the density and basis-set from which they were calculated (RHF = restricted Hartree−Fock, MP2 = second-order Møller−Plesset, B3LYP = Becke's 3-parameter hybrid functional). [c] Source(s) of intramolecular parameters and level of theory at which the cation geometry was calculated. [d] United-atom model also proposed.

organic molecules in aqueous environments in mind) to IL systems is by no means assured. It is also important to remark that, except for the work by Yan et al.,[26] common classical force fields for ionic liquids are nonpolarizable.

Four IL force fields have been published that include specific parametrizations for [dmim]Cl: those of Urahata and Ribeiro[33] (denoted UR, based on the 1-methyl-3-butylimidazolium force field of Morrow and Maginn),[34] Canongia Lopes, Deschamps and Padua (CLDP),[35] Hanke, Price, and Lynden-Bell (HPLB),[36] and Liu, Huang, and Wang (LHW).[37] A summary of the elements of each is given in Table 1. In the case of the alkyl imidazolium ILs, parametrizations for specific torsion potentials are often missing from literature force fields, and fits to ab initio energy calculations or classical normal-mode analysis can be employed to rectify these shortcomings (for example, ref 35). For the LHW force field, the authors go one step further and reparametrize nearly the entire set of force constants for bonds and angles also. Furthermore, the LHW model benefits from the only attempts (to the best of our knowledge) to modify dispersive parameters in order to improve the performance of the IL force field. The authors note, from ab initio gas-phase calculations of the dmim cation with a different anion (PF_6^-), that the close contacts between fluorine atoms of the anion and the unique ring hydrogen (H1) and methyl hydrogens (HM) of the cation are significantly shorter than those observed in molecular mechanics calculations with raw AMBER parameters. Hence, a refined value for σ_{H1} is proposed to reproduce the calculated contact distances more closely. Although similar reasoning could readily be applied to contacts between fluoride atoms and the HM and other ring hydrogens (H2), modifications to the relevant parameters were not attempted by the authors.

Recently, the first ab initio MD study of an ionic liquid was published[38] simulating 8 and 24 ion pair [dmim]Cl systems at 450 K and the experimental density. This was quickly followed by a second investigation by Bühl et al.[39] that cited general agreement with the findings of the first study. It was found that both the center-of-mass cation−anion radial distribution function (RDF) and the 3D anion distribution in ref 38 matched closely those observed by Hardacre et al.[5] Furthermore, it can be shown that, despite consisting of rather different parameters, the available classical models produce similar results. Figure 2 compares the RDFs from ref 38 to those calculated from simulations of 32 ion pairs performed with the DL_POLY[40] software at 450 K and the experimental density. While in the ab initio curve the cation−anion main peak is fairly sharp and

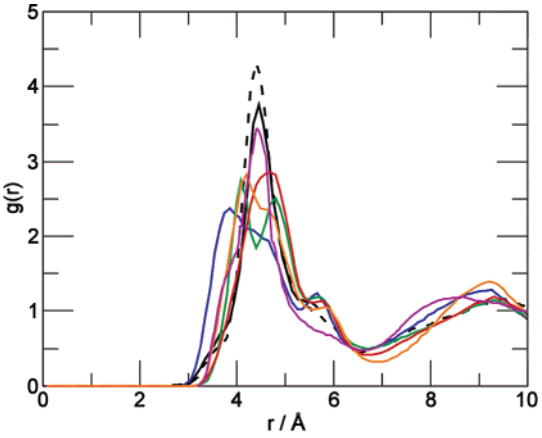

Figure 2. Cation−anion center-of-mass RDFs for the UR (orange), CLDP (red), LHW (green), and HPLB (blue) models compared with those from ab initio MD simulation (solid and dashed black lines for the small and large systems, respectively) and neutron diffraction (purple, reproduced with permission).

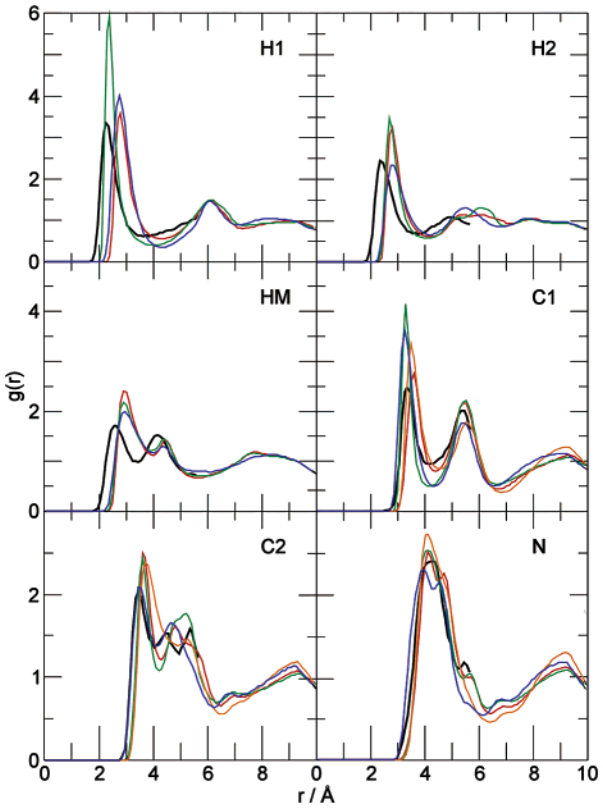

Figure 3. Site−site PRDFs between atoms of the cation and chloride anions for the UR (orange), CLDP (red), LHW (green), and HPLB (blue) models compared with those from ab initio MD simulation (black). Atom types are as shown in Figure 1.

well-defined, the simulated curves tend to be broader and display a more complex structure rather than a single peak. However, generally speaking the agreement is qualitatively good.

More detailed structural data can be elucidated from the ab initio results in the form of atomic site−site partial RDFs (PRDFs) between individual atoms of the cation and the chloride anions. Figure 3 shows these data against those calculated for the classical models for several atom types, and expresses notable differences between the two, chiefly those involving H···chloride contacts (although those involving carbon atoms are predicted particularly well by the Buckingham repulsive potentials employed in the HPLB model). If one is to consider

which interactions in IL systems are the most critical ones then it is reasonable to suggest, in the case of [dmim]Cl, that those between the chloride anion and the (slightly acidic) hydrogen atoms of the imidazolium ring play the most significant role. In fact, the PRDFs given in Figure 3 indicate that this aspect represents a challenge for the force fields commonly used in IL simulation. For the LHW force field, the author's attempts to modify the LJ potential for H1 improve the position of the main peak, but at the expense of an intensity that is rather too high. Certainly, although these models have been successfully used in many studies of the properties and dynamics of IL systems, there are elements within them that will clearly benefit from optimization.

Methods for Force Field Refinement

The force matching method, pioneered by Ercolessi and Adams,[41] provides a technique by which new force fields may be optimized and/or parametrized. Given the configurations (positions and forces) generated by an ab initio MD simulation, a classical force field of fixed functional form may be optimized such that the ab initio forces are reproduced as closely as possible. If the residual error in the forces is small, then a classical trajectory calculated with this force field should sample a more "ab initio-like" region of phase space, producing comparable properties obtained from ensemble averages at a reduced computational effort. This technique has been used only for a handful of systems, not least owing to the scarcity of suitable ab initio MD trajectories, but nevertheless has been successfully applied to a number of systems. For example, atomic potentials have been extracted for Al,[41] Si,[42,43] Si/SiO_2,[44] Ta,[45] and several others (see ref 43 and references therein), as well as molecular force fields for liquid HF[46] and H_2O.[47,48] Indeed, liquid water, in terms of the number of interactions existing in the system, represents the most complicated system tackled by the force matching approach so far.

For [dmim]Cl the ab initio trajectories from ref 38 are available, and may thus be subjected to the force matching approach to generate a more accurate classical force field. In the force matching procedure the cost or objective function that is the subject of minimization is given as

$$\chi^2 = \sum_{x=1}^{C} \sum_{i=1}^{N} (F_i(R_x) - F_i^{\text{model}}(R_x)\{\alpha\})^2 \qquad (1)$$

where $F_i(R_x)$ are individual ab initio force components for a given atom i in a single MD configuration R_x, and $F_i^{\text{model}}(R_x)\{\alpha\}$ are model forces calculated at the same configuration. The sums run over all the N atoms and over a set of configurations C (which can consist of a single configuration). The set of parameters $\{\alpha\}$ contains all the variable components of the force field in the fit, e.g., charges, force constants, etc., which are to be the targets of the minimization. The problem is then to find the set of α that minimizes the objective function (1). Linear minimization is possible provided the variables which are the fitting targets enter linearly (or can be linearized) into the equations for force calculation. Indeed, this direct approach is used by Izvekov and Voth[46,48] where the short-range repulsive force is embodied in a series of interpolated splines, and the atomic charge variables are represented as charge products. The resulting system of linear equations can then be solved by least-squares methods to afford the best-fit to the ab initio data, with the charges recovered through a separate nonlinear method.

Should it be nontrivial (or undesirable) to reduce the force field down to a linear representation, stochastic methods may be readily applied to the problem. A popular method to the solution of this kind of combinatorial optimization is the simulated annealing (SA) approach, which has found use in a diverse number of areas ranging from circuit design[49] to protein folding.[50] Here, a simplex-based SA (SSA) algorithm is employed for the minimization procedure.[51] The force field minimization begins from a randomized set of $\{\alpha\}$ given by

$$\alpha_j = \alpha_j^0 + \lambda(r - 0.5)\alpha_j^0 \qquad (2)$$

where $\{\alpha^0\}$ are initial "guess" parameters, r is a random number between 0 and 1, and λ is a variable defining the degree of randomization (usually 1 or 0.5). An initial fictional temperature T_0 is estimated for these randomized values in the following way. Assuming that each degree of freedom has a harmonic contribution to T_0, the total fictitious temperature is given by evaluating numerically the derivatives of the cost function at different points in parameter space:

$$T_0 = -\frac{1}{M}\sum_{j=1}^{M}\left\langle \alpha_j^0 \frac{\chi^2\{\alpha_j^0 + \Delta\} - \chi^2\{\alpha_j^0 - \Delta\}}{2\Delta} \right\rangle \qquad (3)$$

where the average is evaluated for a sample of α_j^0.

To ensure that a suitably large region of parameter space is explored by the SSA algorithm, this initial value T_0 is multiplied by 10^5 prior to the minimization procedure. The temperature schedule of the SA is defined by an exponential decay of T_0 over 250 steps, reaching a final value of 1, followed by a short zero-temperature "downhill" simplex minimization to settle the set of parameters into the nearest minimum. All α are optimized simultaneously by the simplex method, and the symmetry of the cation is used to reduce the number of variables. However, some additional restraints must be imposed on the procedure. To ensure charge neutrality, the anion is assumed to have a fixed charge of -1 and the cation $+1$, but individual atomic charges within the cation must be allowed to vary independently in the simplex while retaining the imposed total charge. In principle, one could only require the sum of all partial charges to be zero, thus allowing for a fractional charge on anion and cation, as has been done for inorganic molten salts.[52] However, so far most models for IL have used nominal integer charges for anions and cations (one exception is the model of Morrow and Maginn)[34] and we have chosen to follow this philosophy. To impose this constraint, the atomic charge of one atom type (in this case the two nitrogen atoms in the ring) is removed from $\{\alpha\}$, and instead is forced to depend on the other, freely varying charges in the following way

$$2q_{\text{N}} = 1.0 - \sum_{i \neq \text{N}}^{\text{cation}} q_i \qquad (4)$$

Since there is no guarantee that any given minimization will result in the optimal $\{\alpha\}$ (especially given the complex interactions occurring in the IL system under study), a self-consistent statistical approach is introduced. A set of 1000 representative atomic configurations are chosen from those available and a force field is optimized via SSA for every single configuration. This approach can also be applied to fit the forces on a set of configurations, with a concomitant increase in computational cost. In our experience, this did not result in any significant improvement in the quality of results.

Owing to the complexity of the parameter space to be searched, it is not guaranteed that the final resting point of the simplex will be the global minimum, even for very slow annealing schedules. However, elements of the force field that contribute strongly to the total force tend to be rapidly and efficiently located by the algorithm and, for those elements that are repeatedly found to take on similar values, restrictions on the parameter space accessible to the simplex may be imposed. Within a large enough set of fitted force fields (in the region of 500 to 1000), the distributions of parameters can be used to define such limits. Individual α values which show suitably well-defined distributions (i.e., show a small range of highly likely values) may be analyzed by fitting a Gaussian curve to histogram data. Then, the limits $\alpha_j^{\min}$ and $\alpha_j^{\max}$ may be defined as

$$\alpha_j^{\min} = c_j - \lambda w_j; \qquad \alpha_j^{\max} = c_j + \lambda w_j; \qquad \lambda = 0.5 \quad (5)$$

where c_j and w_j are the center and width of the Gaussian fit to the parameter distribution of α_j. The cost function (1) is then modified to incorporate a quadratic restraint upon any value of α_j that wanders outside of the defined window and becomes

$$\chi^2 = \sum_{x=1}^{C}\sum_{i=1}^{N}(F_i(R_x) - F_i^{\text{model}}(R_x)\{\alpha\})^2 + \sum_{x=1}^{C}\sum_{j=1}^{M}\chi_{\text{res}}{}^2(\alpha_j)$$

$$\chi_{\text{res}}{}^2(\alpha_j) = \begin{cases} 0, & \alpha_j^{\min} < \alpha_j < \alpha_j^{\max} \\ |\alpha_j - \alpha_j^{\min,\max}|^2\,\chi^2 & \text{otherwise} \end{cases} \quad (6)$$

The use of the current χ^2 value calculated from (1) as the "force constant" in $\chi_{\text{res}}{}^2(\alpha_j)$ results in fairly strong penalties being enforced, but also allows such limits to be imposed with a strength that adjusts as the SSA progresses. This prevents $\chi_{\text{res}}{}^2$ from dominating the total χ^2 value in the later stages of the minimization, thus reducing a possible bias introduced by the restraint procedure.

With a set of parameter limits defined, new restricted SSA (RSSA) runs are then conducted on the individual configurations generating a new set of parameter distributions. Gaussians are fit to the resulting histograms and new (hopefully better) restraints are imposed, and so on. Repetition of this "self-consistent" process continues until all the parameter distributions are sufficiently narrow, and the force field parameters have "converged". For the restraint procedure to be meaningful, it is important to check that the final distributions are narrower than the limits imposed, and not artificially forced.

Proof of Concept

Validation of the proposed method proceeds by attempting to recover the force field of a classical simulation, for which an exact solution is known and $\chi^2 \rightarrow 0$. A classical trajectory of 8 [dmim]Cl ion pairs in a cubic cell was generated in the NVT ensemble at the experimental density. A typical IL force field was created from classical parameters taken from the OPLS-AA force field, excepting the LJ for chloride which were taken from fits to Born−Mayer data.[53] This set of parameters constitute $\{\alpha^0\}$ in the SSA calculation and will be referred to as the OPLS/Tosi force field later in the text. Simulations were conducted at 450 K and the experimental density of 1.095 g cm^{-3},[6] using a time step of 0.5 fs. Electrostatics were treated by the standard Ewald method. Every 25th configuration was taken from a single trajectory of 25000 to give a representative set of 1000, and SSA was performed for each as described above. The MD force field consisted of six unique bond terms, nine angles, five torsions, six LJ atom types, and eight charges giving a total of 51 variables, the full potential energy expression being

$$E = \sum_{\text{bonds}}\frac{k_{\text{bond}}}{2}(r - r_0)^2 + \sum_{\text{angles}}\frac{k_{\text{angle}}}{2}(\theta - \theta_0)^2 + \sum_{\text{torsions}}\frac{k_{\text{torsion}}}{2}(1 + \cos(n\phi - \phi_0)) + \sum_{i<j}4\epsilon_{ij}\left(\left(\frac{\sigma_{ij}}{r_{ij}}\right)^{12} - \left(\frac{\sigma_{ij}}{r_{ij}}\right)^{6}\right) + \sum_{i<j}\frac{q_i q_j}{r_{ij}} \quad (7)$$

The last two terms operate only between nonbonded atoms, or pairs of atoms separated by at least three bonds. If the separation is exactly three bonds then a scaling factor of 0.5 is introduced to the potential. While all of these parameters are correlated to a degree, some are much more strongly coupled than others, notably the force constants of the internal angles of the imidazolium ring. These three degrees of freedom are reduced to a single common force constant in $\{\alpha\}$, since in the classical simulation the three values of k_{angle} are identical.

Since the optimal solution is known it is possible to define an average error parameter ∂ between the exact force field values (or a subset of them) and those derived from SSA:

$$\partial = \frac{1}{M}\sum_{j=1}^{M}\left|\frac{\alpha_j^0 - \alpha_j}{\alpha_j^0}\right| \quad (8)$$

The value of ∂ is therefore zero for an exact match and 1 if α_j are either all zero or twice α_j^0. Figure 4, panels 1a−4a, shows the obtained parameter distributions for four types of force field parameter (bond force constants, angle force constants, atomic charges, and LJ ϵ) while Table 2 lists the ∂ values. For the force constants, pronounced and well-defined peaks are visible for each indicating definite regions of "high probability" parameter space and allowing restraints to be imposed on them with confidence. The accuracy in the positions of the peaks of these distributions is reflected in the ∂ values, which are close to zero. For the atomic charges, although some peak structure can be seen it is clearly more difficult to define any regions of high probability with any certainty. Consequently, the ∂ value is high, and only two of the six parameters in this part of the force field may be subsequently restrained. LJ ϵ show no meaningful peak structure in the distributions whatsoever, since all have clustered around zero (leading to $\partial = 1$) and display long "tails" of force field values stretching over a wide numerical range. This is characteristic of parameters whose contributions to the force are being drowned out by other, stronger elements, and consequently attain values that are intuitively nonsensical. Since it is difficult to bias force contributions from specific force field elements in order to place them on an equal footing, this issue is not easy to directly resolve. One possibility would be to run simulations where the stronger force components are eliminated by appropriate geometrical constraints such as rigid rings. However, such a simulation is not useful per se, and it may be preferable to use a few selected configurations (e.g., from the solid structure) for the force matching procedure, thus avoiding a lengthy simulation of little use.

SA algorithms are principally employed because of their ability to navigate over hills or barriers of high "energy", allowing local minima to be traversed safely without becoming

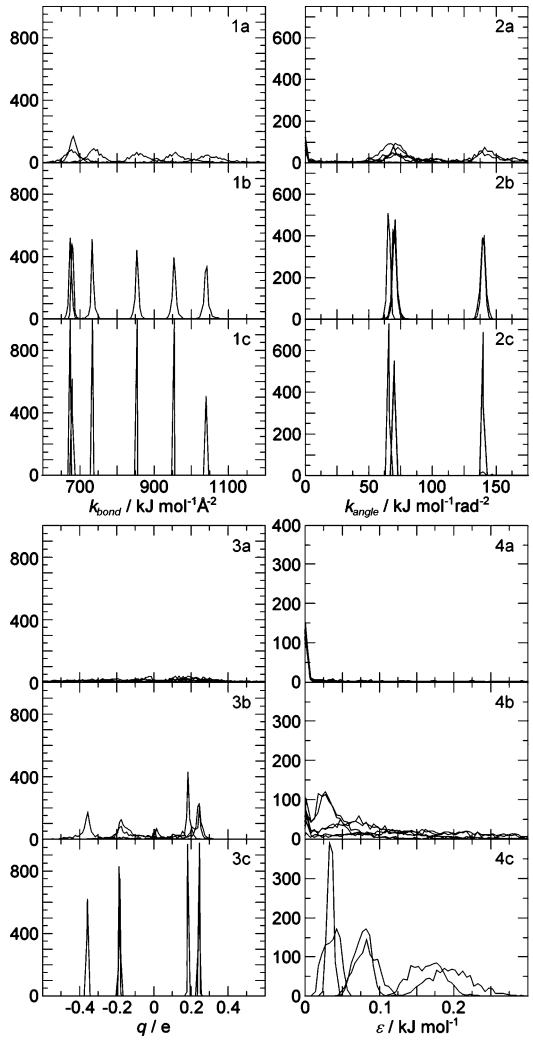

Figure 4. Simplex simulated annealing results for bond and angle force constants, atomic charges, and LJ ϵ values for the classical system. Shown are initial SSA (1a-4a), first RSSA (1b-4b) and final restrained minimization parameter distributions (1c-4c). Individual curves are not labeled with the force field parameters they represent, the intention being to highlight general trends in the evolution of distributions.

trapped, and increasing the chance of the global minimum being located. Yet, the enormously complex landscape related to the systems of parameters subject to minimization in this work means location of the global minimum is sufficiently unlikely for it to be considered unobtainable. This is mostly due to different elements within $\{\alpha\}$ showing markedly different contributions to the atomic forces—in the broadest sense, the strong *intra*molecular and weak *inter*molecular contributors. For a given atomic configuration, the contributions to the total forces on the atoms from individual force field components may be calculated. Averaging these values over the configurations of a classical trajectory reveals the following percentage contributions for [dmim]Cl: bonds (45.6%) > angles (29.9%) ≫ charges (9.5%) > torsions (7.9%) ∼ LJ (7.1%). Hence, the direction of the search conducted by the simplex tends to be driven by the stronger elements of the intramolecular bond and angle terms. It then transpires that the optimal set of strong parameters is readily found by the algorithm (independent of the starting position) but the subset of weaker parameters is liable to suffer. Such a situation can be visualized as a large, fairly regular "basin of attraction" defined by the intramolecular parameters, upon which is etched a complex, irregular landscape defined by the intermolecular part. Thus, unless the strong elements are reasonably well-defined the weak elements are unlikely to be found—a small error in a single strong force field parameter will tend to propagate into large errors in weak force field parameters, hence the strange results for the LJ ϵ seen in Figure 4, panel 4a. Thus, before these weaker elements may be determined with any certainty, the strong contributors to the force must be reasonably well defined.

From the SSA results on the classical [dmim]Cl configurations 33 of the 51 parameters were suitable for restraint (only four of which are relevant to the intermolecular forces). An RSSA run now begins from this point. The procedure is the same as for SSA, but instead using the modified cost function (6). Initial randomization of the starting $\{\alpha\}$ for each minimization differs slightly with regard to the restrained parameters, whose starting values are randomly selected from within the two restraint limits. Results from this first RSSA run are shown in Figure 4, panels 1b−4b. Both bond and angle force constants now show much sharper and cleaner distributions, accompanied by reductions in their respective ∂ values. Hence, further restraints based on these data will limit these parameters to an even smaller window. Distributions of the atomic charge parameters are improved to a degree that allows all of them to be restrained in the next RSSA calculation, despite a mild tendency toward zero that has the effect of creating asymmetric distributions. The most remarkable transformation, however, is in the LJ ϵ that before offered no useful information, but which now clearly suggest values for the force field parameters. After two further RSSA runs the distributions are essentially converged, but may be improved slightly through the use of a short Simplex-driven minimization of the parameters employing the best set of restraints obtained from the RSSA calculations. It was found that simple minimization schemes (i.e., without restraints) produced only mediocre results owing to their inability to overcome local minima. However, here it is prudent to take advantage of downhill minimization since a limited region of parameter space can be defined by the RSSA-derived restraints. Following this final minimization (Figure 4, panels 1c−4c, and denoted RSSA-Z in Table 2), the average $\log(\chi^2)$ value has been reduced to ∼3.4, equivalent to an average error of around 10 J mol^{-1} A^{-2} (<0.1%) per force vector per atom. This small residual force is a result of the high correlation and mutual compensation present between the bond and angle terms within the ring, also affecting the internal torsional component of the force field. Nevertheless, the original force field has to all intents been reclaimed through the use of the (R)SSA method.

TABLE 2: Individual Parameter Type Errors (∂) for the Classical SSA and RSSA Calculations

run	k_{bond}/r_0	k_{angle}/θ_0	$k_{torsion}$	σ	ϵ	q	$\langle\log(\chi^2)\rangle$
SSA	0.007/0.003	0.017/0.008	0.065	0.549	1.000	0.405	7.596
RSSA-1	0.000(2)/0.001	0.002/0.004	0.174	0.011	0.141	0.080	5.866
RSSA-2	0.001/0.002	0.001/0.002	0.017	0.007	0.051	0.006	4.407
RSSA-3	0.002/0.002	0.001/0.002	0.007	0.005	0.056	0.007	3.991
RSSA-Z	0.002/0.002	0.002/0.001	0.010	0.008	0.161	0.007	3.409

Optimization of a [dmim]Cl Force Field from ab Initio Data

The eight ion pair density functional theory (DFT) trajectory of ref 38 provides approximately 50000 sets of fully ab initio forces and the associated atomic positions. This database was stripped down so it contained only every 25th configuration, and from these 1000 configurations were selected. It is noted at this point that simply producing a refined set of intermolecular parameters would suffice, since these may justifiably be considered the most important terms in the force field. However, the fully flexible nature of the underlying ab initio simulation necessitates that both intra- and intermolecular parts are fit simultaneously. Again, a DFT trajectory employing rigid cations would allow fitting of a purely intermolecular force field. On the other hand, it is also desirable to assess the quality of the current stock of intramolecular parameters used in IL simulations.

In the previous SSA, the fitted force field contained the specific terms used to perform the initial MD. Here, it is unknown whether certain apparently "identical" features of the cation, for example, the C1−H1 and C2−H2 bond force constants and equilibrium distances, can safely be represented by a single term in the force field. Therefore a larger number of parameters was subjected to the fit to allow for possible variations (the symmetry of the cation was still employed, however). Hence the force field consists of seven bond, ten angle, and ten torsion terms, eight atom types giving eight pairs of LJ parameters, and eight atomic charges, for a total set of 66 variables, and is of the same functional form as (7). SSA simulation parameters are those specified for the classical trajectory above, with the exception of λ in (2) which is set to 0.5.

Initial results for several parameter types from the first SSA runs are shown in Figure 5, panels 1a−4a. The immediate impression on comparison with the SSA results in Figure 4 is that there is far more noise and uncertainty in the parameter distributions for the ab initio system. Nevertheless, those that are better-defined certainly show a Gaussian-like shape—for the bond and angle k it is possible to define a centerpoint for each of the parameter distributions and to extract new force field parameters. For the atomic charges and LJ ϵ, though, there are definite similarities with the initial SSA results of the classical fit, with the former showing wide dispersal of parameters and the latter no useful structure at all. Applying progressive restraint runs (Figure 5, panels 1b−4b) it quickly becomes apparent that the "rate of convergence" of the force field parameters is slower than was observed for the classical test. After several RSSA calculations the distributions can be significantly improved, and after a final short restrained minimization the result is, by and large, a set of clean (although occasionally broad) parameter distributions (Figure 5, panels 1c−4c) for both inter- and intramolecular parts of an IL force field from which parameter values can confidently be read. The average $\log(\chi^2)$ value from this last result is ∼7.6, equating to an average error per force component per atom of around 1300 J mol^{-1} A^{-2} and reproducing the ab initio forces to within 2%, 1 order of magnitude larger than the 0.1% obtained for the classical model.

Results and Discussion

Optimized [dmim]Cl force field parameters may be found in Tables 3 and 4. First inspection reveals that the intramolecular parameters require some attention, since the equilibrium angles are significantly higher or lower than might be expected. This is best exemplified by considering the internal ring angles which

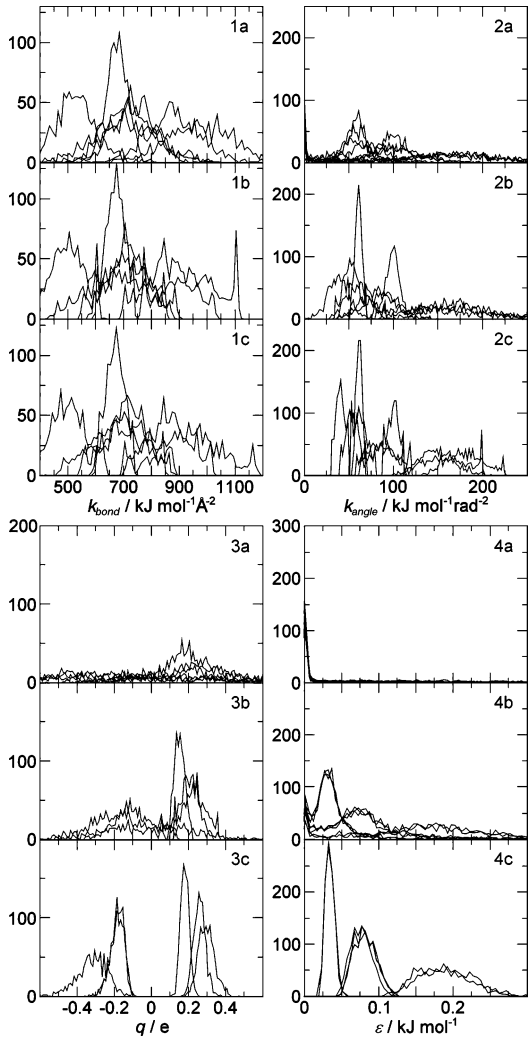

Figure 5. Simplex simulated annealing results for bond and angle force constants, atomic charges and LJ ϵ values for the ab initio system. Shown are initial SSA (1a−4a), first RSSA (1b−4b), and final restrained minimization parameter distributions (1c−4c). Individual curves are not labeled with the force field parameters they represent, the intention being to highlight general trends in the evolution of distributions.

one would normally expect to sum to 540°, but which here total 689°. Clearly this is absurd taken in a literal sense, but in simulation the net effect of these high equilibrium angles will be simply to generate extra force around the imidazolium ring, perhaps making up for a source of ring strain not accounted for in the classical model. In tests during the RSSA runs, restricting these parameters to their "expected" regions proved highly detrimentory to other parameters, but it is likely that a more elaborate force field, perhaps one that includes terms specific to the conjugated system in question, will alleviate the problem and return the equilibrium angles to more expected values. On the other hand, it may be that correlation between these three ring angles (and their force constants) is enforcing a somewhat different effect from that observed in the classical tests, beyond a simple first-order compensation. These two possibilities certainly warrant further attention, but for the purposes of this work these parameters are left as-is, since MD of isolated cations proved that their geometry is not adversely affected by these values. The effect on the atomic forces, though, must be considered a necessary and positive one.

Force constants for bond, angle and torsions within the model do not move far from those found in the OPLS (and other) force

TABLE 3: Optimized Lennard-Jones and Intramolecular [dmim]Cl Potential Parameters As Obtained via Force Matching

atom type	σ_{ii}/Å	ϵ_{ii}/kJ mol^{-1}	atom type	σ_{ii}/Å	ϵ_{ii}/kJ mol^{-1}
H1	1.172	0.142	**C1**	3.842	0.336
H2	1.363	0.139	**C2**	3.695	0.338
HM	1.407	0.141	**CM**	3.657	0.316
N	3.176	0.802	**Cl**	3.541	0.757

bond	r_0/Å	k_{bond}/kJ mol^{-1} Å^{-2}	bond	r_0/Å	k_{bond}/kJ mol^{-1} Å^{-2}
N−C1	1.341	3594.6	**C1−H1**	1.107	2821.7
N−C2	1.400	2987.2	**C2−H2**	1.104	3020.2
N−CM	1.473	2098.6	**CM−HM**	1.119	2810.6
C2−C2	1.409	3934.4			

angle	θ_0/deg	k_{angle}/kJ mol^{-1} rad^{-2}	angle	θ_0/deg	k_{angle}/kJ mol^{-1} rad^{-2}
N−C1−N	132.5	656.5	**N−C1−H1**	107.3	226.5
C1−N−C2	141.0	619.1	**N−C2−H2**	98.0	220.6
N−C2−C2	137.4	751.8	**C2−C2−H2**	94.8	168.9
C1−N−CM	113.8	463.8	**N−CM−HM**	104.4	418.6
C2−N−CM	116.0	494.8	**HM−CM−HM**	103.4	256.9

torsion	$k_{torsion}$/kJ mol^{-1}	ϕ_0/deg	n	torsion	$k_{torsion}$/kJ mol^{-1}	ϕ_0/deg	n
N−C1−N−CM	19.9	180.0	2	**H2−C2−N−CM**	8.3	180.0	2
H1−C1−N−CM	7.5	180.0	2	**C2−C2−N−CM**	20.6	180.0	2
H2−C2−C2−H2	12.4	180.0	2	**H2−C2−N−C1**	20.6	180.0	2
C*−N−CM−HM	0.0	180.0	3	**H2−C2−C2−N**	21.1	180.0	2
H1−C1−N−C2	18.4	180.0	2	**internal ring**	4.7	180.0	2

TABLE 4: Optimized Atomic Charges for [dmim]Cl As Obtained via Force Matching, Along with Those Presented in Other Models

	q/e				
atom type/group	this work	CLDP	LHW	HPLB	UR
H1	0.293	0.210	0.233	0.097	
H2	0.259	0.210	0.248	0.094	
HM	0.180	0.130	0.109	0.064	
N	0.133	0.150	0.059	−0.267	−0.399
C1	−0.181	−0.110	−0.008	0.407	0.605
C2	−0.176	−0.130	−0.171	0.105	0.241
CM	−0.311	−0.170	−0.074	0.124	0.355
Cl	−1.000	−1.000	−1.000	−1.000	−1.000
CH1[a]	0.112	0.100	0.225	0.504	0.605
CH2[b]	0.083	0.080	0.077	0.199	0.241
CHM[c]	0.229	0.220	0.253	0.316	0.355

[a] Sum of charges C1 and H1. [b] Sum of charges C2 and H2. [c] Sum of charges CM and 3×HM.

TABLE 5: Local Dipoles Calculated at the Centers-of-Mass of Aromatic C−H Bonds in the dmim Cation at the Average Geometry Observed in the ab Initio MD Simulations in Reference 38

	μ/Debye			
bond	this work	CLDP	LHW	HPLB
C1−H1	1.531	1.089	1.161	0.312
C2−H2	1.352	1.091	1.296	0.421

fields, which may be taken as some vindication for the derivation of parameters from gas-phase calculations. It is interesting to note, however, that k_{bond} values are all lower than those in OPLS, suggesting general overestimation by the force field. Not without reason, force constants related to C−H bonds change the least since these are arguably one of the simplest and most well-characterized elements in any classical force field. It is prudent to mention here the work of Liu, Huang, and Wang,[37] who reparametrized force constants with the aid of gas-phase frequency calculations. For the most part, the values they suggest follow the general trend of decreasing with respect to the OPLS literature values, and in one or two cases are extremely close to those given here. For example, the force constant of the N−C2 bond is given as 3573 kJ mol^{-1} in the OPLS force field, and LHW adjust this to 3012 kJ mol^{-1} compared to the optimized value here of 2987 kJ mol^{-1}. The same is also true for angle force constants, although the uncertainties associated with the internal ring angles in this case make a direct comparison difficult. Trends in the torsion angle force constants are less clear, but again this may be a result of internal ring angle correlation.

In the intermolecular part of the force field it is observed that the LJ ϵ values increase slightly with respect to the OPLS/Tosi values by 10−25%. For the LJ σ two distinct patterns emerge. First, the radii of all types of hydrogen atoms in the cation *decrease* to roughly half of the OPLS values. Second, the radii of the carbon atoms *increase* by 0.1−0.3 Å. The remaining N and chloride radii decrease by ∼0.08 Å (cf. OPLS) and ∼0.23 Å (cf. fits to Born−Mayer potentials).[53] The first of these trends is in line with the findings of Liu et al. for H1, although the decrease in this work is around 0.6 Å larger. Atomic charges and group sums, Table 4, decrease slightly with respect to those calculated with the RESP method at the HF/6-31G* level, but remain among the largest of the classical models listed signifying the presence of a greater degree of electrostatic interaction. Most similarity is seen with the CLDP values, particularly with regard to the summed C−H data which are almost identical, suggesting that the derivation of atomic charges from gas-phase ab initio data is an economic and useful approximation in the majority of cases where liquid data are not available. In line with the increased charges it is observed that the local dipoles on the C−H bonds (Table 5) are the largest observed for the models. This certainly seems to be an indication of the polarization of these bonds in the liquid state, but which may only be properly accounted for by a more complex potential.

The performance of the potential in production MD simulations was assessed through NVT (conducted at the experimental density) and NPT calculations of 32 [dmim]Cl ion pairs at 450 K. It is found that the density of the force field is 1.25 g cm^{-3}, higher than both the experimental value of 1.11 g cm^{-3} and the values predicted by other force fields which lay within 1−5% of this figure. The principal reason for this is linked to the significant reductions in some σ values, necessary to reproduce

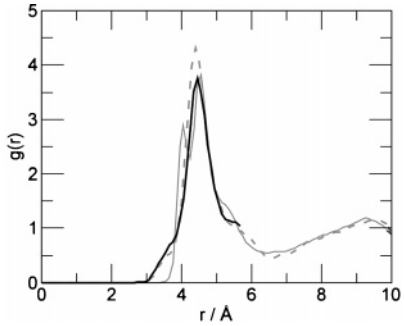

Figure 6. Cation−anion center-of-mass RDFs for the optimized classical potential (thin solid line) compared with those from ab initio MD simulation (thick solid and dashed lines for the small and large systems, respectively).

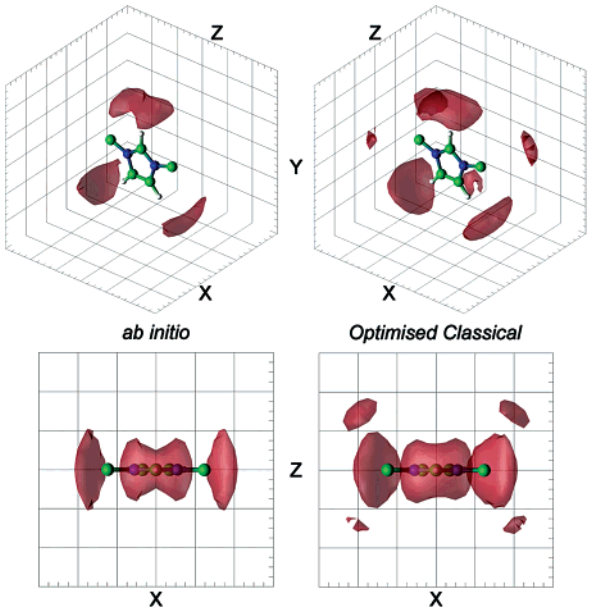

Figure 7. Three-dimensional distributions of anions about a given cation for the optimized classical model and ab initio MD simulations. Lobes represent density of 0.03 Å^{-3}, equivalent to six times the average density of chloride ions. Grid spacing is 2 Å.

well the structure of the liquid but also enforcing a slight contraction in the volume of the system. This may be an influence of the ab initio system, for which the DFT-simulated density was not assessed but which may also be too high (in line with typical trends of usual approximations in DFT) and which is carried across into the classical force field through the force matching process. Figure 6 shows the calculated cation−anion RDF against the ab initio results from ref 38, where it can clearly be seen that the agreement is excellent. Main peak position and intensity are reproduced well by the optimized potential, excepting the addition of a small shoulder at 4 Å that suggests more detailed structuring than was observed by ab initio simulation. The three-dimensional distribution of anions about a given cation also reflects this accuracy, Figure 7, agreeing with the observed regions of high probability in the ab initio simulations given in ref 38. In particular, no density is observed above and below the plane of the ring, and no density hole is observed in the lobe directly above the axis of the C1−H1 bond. At this density level lobes about the methyl hydrogens have also begun to appear, again suggesting that the optimized force field produces more structured distributions than the ab initio calculations.

For the PRDFs, Figure 8, peak positions are excellent, with those involving hydrogen atoms showing particular improvement

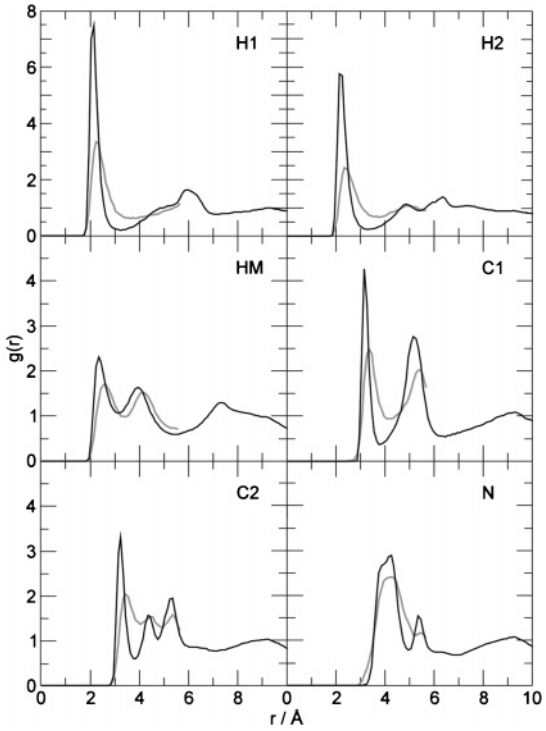

Figure 8. Site−site PRDFs between atoms of the cation and chloride anions for the optimized classical potential (black line) compared with those from ab initio MD simulation (grey line). Atom types are as shown in Figure 1.

over the previous classical results, and a much richer structuring of anions about C2 is now clear with all three peaks of the ab initio trace faithfully reproduced by the new model. However, these classical PRDFs are characterized by rather high peak intensities, and the suggestion of more detailed structuring is borne out here also. Such features could be explained if the system had become trapped in, for example, a glassy state, but since diffusion coefficients calculated for this simulation and those of the other classical models are of the same order of magnitude (that of the UR model is approximately equal to the value observed in this work), this seems not to be the case.

Combining the effects of increased carbon radii with decreased hydrogen radii has the net result that the collision diameters of all hydrogens in the molecule are within those of their respective carbons—in effect, the hydrogen nuclei have been subsumed into their bonding neighbors. For example, the zero-crossing point of the C1···chloride LJ interaction occurs at 3.69 Å, while that for H1···chloride occurs within this boundary at 3.44 Å (taking into account the C1−H1 bond) hence the influence of hydrogen atoms on the chloride appears largely restricted to electrostatics. Performing short MD simulations using the optimized force field, but where the C1 and H1 σ have been reset to the OPLS values, produces site−site RDFs for these atoms that resemble strongly those of the other LJ force fields shown in Figure 3. Subsequently changing the C1 radius to the optimized value has little effect on the PRDFs, but immediately as the same is done for the H1 radius the sharp intensities of the PRDFs return. Performing the same simulations for C2/H2, it is important to note that the characteristic three-peak C2···chloride PRDF structure is not seen until the H2 radius is optimized. Thus it appears that the distribution of anions about the C2 position depends on the absence of a repulsive H2···chloride interaction. It is possible to infer from this that the force matching process can find little use for H···chloride repulsions, and has subsequently minimized them

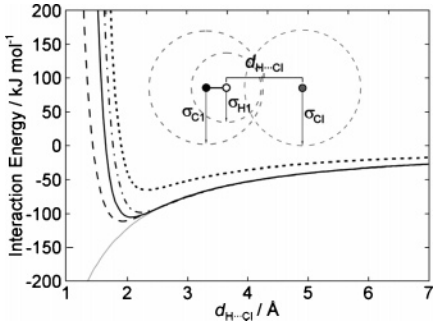

Figure 9. Calculated intermolecular interaction energies for an idealized C1−H1···chloride contact. Shown is the total interaction energy calculated by using the optimized parameters (solid black line), the Coulombic component of this energy (gray line), systems where LJ contributions from H1 are removed (black dashed line) and all LJ ϵ have been multiplied by 2 (black dot−dashed line), and the original OPLS/Tosi interaction (black dotted line).

through these reductions in σ. Even so, since the distributions for these parameters are still well-defined there may be some small yet important force that can be provided by the inclusion of such interactions.

Figure 9 shows the intermolecular interaction energy calculated for an ideal C1−H1···chloride contact using the OPLS/Tosi and optimized force field values. Not only has the minimum shifted to lower distances (as would be necessary to correctly reproduce the peak positions in the PRDFs) with respect to the OPLS curve, it is also markedly lower in energy. Likely this is an indication of the optimized force field attempting to provide a more realistic potential between hydrogen and chloride atoms, within the limitations imposed by the specific functional form. Intermolecular energy curves where repulsive H1···chloride elements have been removed (black dashed line) and where all ϵ have been increased by a factor of 2 (black dot−dashed line) are also shown in Figure 9. Where it might have been expected that disregarding H1···chloride repulsions would have little effect on the energy profile, given the findings outlined earlier, there is evidently a nontrivial contribution from this repulsion, despite the reduced radius of the atom. The position of the minimum is shifted to an even shorter distance, now determined by the C1···chloride repulsion, and accompanied by a small lowering of the energy. It may well be expected that a similar shift will occur when increasing the ϵ values, since the attractive well of the LJ potential will be made deeper. However, the opposite behavior is observed, with the minimum moving to slightly higher energy and longer distance, due to the increased strength of the dominant repulsive interaction. This rather counter-intuitive behavior has the effect of reducing slightly the strength of interaction between the cation and anion, which potentially may affect the structural properties of the liquid. Short MD simulations where all ϵ have been modified in this way show that this is indeed the case, with PRDFs matching even more closely those from ref 38, Figure 10.

It should be recognized, though, that from the point of view of force matching optimization this is a step away from the "optimal" potential in the sense that this modified force field has associated with it a χ^2 larger than that of the optimized set of parameters, Figure 11. We also observe here that the optimized force field corresponds to a χ^2 value toward the higher extremes of the SSA distributions, which brings into question the validity of taking the Gaussian centers of parameter distributions in order to ascertain their force field value. However, examining those results that represent the lower 10% of the SSA distribution where $\log(\chi^2) = 7.3-7.5$, and again

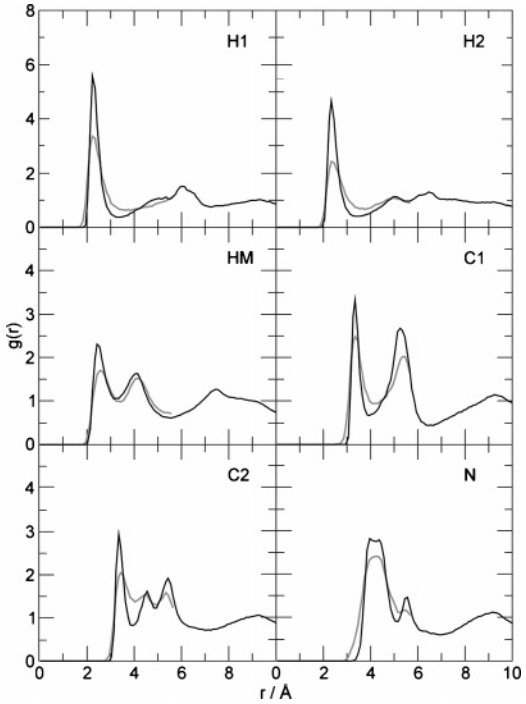

Figure 10. Site−site PRDFs between atoms of the cation and chloride anions for the optimized classical potential with all ϵ multiplied by a factor of 2 (black line) compared with those from ab initio MD simulation (gray line). Atom types are as shown in Figure 1.

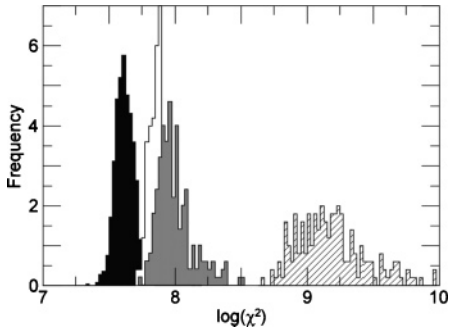

Figure 11. Normalized histogram distributions of the $\log(\chi^2)$ value as obtained from the SSA minimization procedure on the ab initio data (black), the optimized model so obtained (white), the optimized model where epsilons have been modified (gray), and the OPLS/Tosi model (crosshatched).

fitting a force field to the resulting parameter distributions, it is observed that most terms are essentially unchanged (despite some distributions being rather too noisy to obtain a good fit). Indeed, intermolecular terms derived from this subset of force fields are almost identical—applying (8) using the terms in Table 3 as the expectation values α_j^0 yields $\partial = 0.019$. Ultimately this suggests that interplay between intramolecular terms is the cause of the phenomenon, although whether the high correlation between parameters or the simple method used to extract them is to blame is unclear.

A more physical description of the differences between classical force fields and the ab initio results can be obtained through considering the absolute value of the force, $|F|$, on the chloride anions, Figure 12. Moreover, a more critical evaluation of the intermolecular terms is possible since there are no intramolecular contributions to the force on this ion. Clearly, the OPLS/Tosi force field produces a wide spread of values in contradiction to the distribution found within the ab initio simulation, indicating that typical IL force fields such as this do not model well the forces felt by the chloride anions in MD

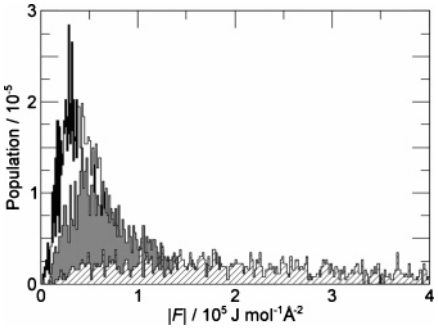

Figure 12. Normalized histogram distributions of the absolute value of the force on the chloride atoms as calculated in ref 38 over 200 configurations of the DFT trajectory (black). Also shown are classically calculated forces at the same configurations from the optimized (white), optimized with modified ϵ (gray), and OPLS/Tosi (crosshatched) force fields.

simulation. The optimized set, however, resembles much more closely the DFT-calculated data indicating that the force matching procedure has successfully improved the intermolecular force field with respect to the supplied classical terms. For the modified ϵ the distribution is shifted slightly further away from that of the ab initio—as has already been discussed, this is due to the original set of optimized values minimizing the residual force, and sacrifices accuracy of the chloride forces for better structural features.

Conclusions and Outlook

A new method for the optimization of classical MD force fields of general functional form through the use of force matching has been presented, and has yielded an improved potential for [dmim]Cl based on the ab initio MD simulation data of ref 38. While the optimized force field reproduces well the ab initio site−site partial RDF data in terms of peak position, the peaks themselves are rather too intense suggesting that some over-structuring may be present in the classical MD simulation. Simple manipulation of the LJ ϵ values results in a significant improvement of the PRDFs, with peak heights reducing and peak positions shifting slightly toward longer distances, providing even better agreement with the ab initio data. Our chloride anion force distributions show that the force matching method indeed improves the atomic forces with respect to the ab initio simulation, suggesting that the overstructuring effect may be attributed to limitations of the imposed functional form.

Since these ϵ do not provide the lowest amount of residual force, they were not located as optimal by the force matching algorithm. Thus, while the best set of parameters is found that minimizes the residual force, since the latter is not extremely small this does not necessarily correspond to a force field that gives the best representation of the liquid structure as measured by PRDFs. Nevertheless, the PRDFs are significantly improved in the original optimized force field and, since the integration of such data into the cost function driving the minimization is nontrivial because it is an ensemble-average property, the fact that it is not necessary to specifically request its reproduction by the optimized potential is a considerable advantage.

The force field provided by the method, as has been briefly demonstrated here, predicts structural data in-line with that of the ab initio simulations. Examining the force field parameters, though, it is clear that some questions still remain to be answered. First of all, releasing the constraint of using nominal integer charges for anions (−1) and cations (+1) may improve the situation because smaller charges can be compensated by smaller ϵ. It is also known that, for nonpolarizable force fields, smaller partial charges are required to reproduce dynamical properties of solid and molten inorganic salts such as NaCl.[52]

We observe "unnatural" intramolecular equilibrium angles for the imidazolium ring that appear to be generating extra force on behalf of some phenomena which are not described in the force field. For the intermolecular part a new set of LJ and charge parameters have been generated, and it is fairly reasonable to consider these as a separate entity from the intramolecular part in the context of MD simulation. However almost certainly given the propensity for hydrogen bonding within alkylimidazolium halide ILs,[54] it seems unlikely that a simple LJ potential can describe well the complex network of interactions occurring within these systems. The method presented here will thus be further employed as an investigative tool, assessing the performance of other functional forms of the intermolecular terms in the description of IL systems. Correlation between intramolecular terms will be examined in order to try and resolve the effect of this on the extraction of final parameters. This section of the force field will also be extended in an attempt to account for the extra force distributed about the imidazolium ring.

Acknowledgment. This work was funded by the EPSRC, grant nos. EP/D029538/1, GR/S41562/01, and GR/S18106/01. We also thank P. Ballone and R. M. Lynden-Bell for useful discussions.

References and Notes

(1) Paulechka, Y. U.; Zaitsau, D. H.; Kabo, G. J.; Strechan, A. A. *Thermochim. Acta* **2005**, *439*, 158.
(2) Paulechka, Y. U.; Kabo, G. J.; Blokhin, A. V.; Vydrov, O. A.; Magee, J. W.; Frenkel, M. *J. Chem. Eng. Data* **2003**, *48*, 457.
(3) Welton, T. *Coord. Chem. Rev.* **2004**, *248*, 2459.
(4) Chiappe, C.; Pieraccini, D. *J. Phys. Org. Chem.* **2005**, *18*, 275.
(5) Hardacre, C.; Holbrey, J. D.; McMath, S. E. J.; Bowron, D. T.; Soper, A. K. *J. Chem. Phys.* **2003**, *118*, 273.
(6) Fannin, A. A.; Floreani, D. A.; King, L. A.; Landers, J. S.; Piersma, B. J.; Stech, D. J.; Vaughn, R. L.; Wilkes, J. S.; Williams, J. L. *J. Phys. Chem.* **1984**, *88*, 2614.
(7) Yang, Z.; Pan, W. B. *Enzyme Microb. Technol.* **2005**, *37*, 19.
(8) Wakai, C.; Oleinikova, A.; Ott, M.; Weingartner, H. *J. Phys. Chem. B* **2005**, *109*, 17028.
(9) Heintz, A.; Verevkin, S. P. *J. Chem. Eng. Data* **2005**, *50*, 1515.
(10) Harris, K. R.; Woolf, L. A.; Kanakubo, M. *J. Chem. Eng. Data* **2005**, *50*, 1777.
(11) de Azevedo, R. G.; Esperanca, J.; Najdanovic-Visak, V.; Visak, Z. P.; Guedes, H. J. R.; da Ponte, M. N.; Rebelo, L. P. N. *J. Chem. Eng. Data* **2005**, *50*, 997.
(12) de Azevedo, R. G.; Esperanca, J.; Szydlowski, J.; Visak, Z. P.; Pires, P. F.; Guedes, H. J. R.; Rebelo, L. P. N. *J. Chem. Thermodyn.* **2005**, *37*, 888.
(13) Deschamps, J.; Padua, A. A. H. Interactions of gases with ionic liquids: Molecular simulation. In *Ionic Liquids Iiia*: *Fundamentals, Progress, Challenges, and Opportunities, Properties and Structure*; American Chemical Society: Washington, DC, 2005; p 150.
(14) Kumelan, J.; Kamps, A. P. S.; Urukova, I.; Tuma, D.; Maurer, G. *J. Chem. Thermodyn.* **2005**, *37*, 595.
(15) Hanke, C. G.; Atamas, N. A.; Lynden-Bell, R. M. *Green Chem.* **2002**, *4*, 107.
(16) Hanke, C. G.; Lynden-Bell, R. M. *J. Phys. Chem. B* **2003**, *107*, 10873.
(17) Wu, X. P.; Liu, Z. P. *Wuli Huaxue Xuebao* **2005**, *21*, 1036.
(18) Lynden-Bell, R. M.; Kohanoff, J.; Del Pópolo, M. G. *Faraday Discuss.* **2005**, *129*, 57.
(19) Lynden-Bell, R. M. *Mol. Phys.* **2003**, *101*, 2625.
(20) Chaumont, A.; Wipff, G. *Phys. Chem. Chem. Phys.* **2005**, *7*, 1926.
(21) Chaumont, A.; Wipff, G. *J. Phys. Chem. B* **2004**, *108*, 3311.
(22) Pinilla, C.; Del Pópolo, M. G.; Lynden-Bell, R. M.; Kohanoff, J. *J. Phys. Chem. B* **2005**, *109*, 17922.
(23) Jorgensen, W. L.; Maxwell, D. S.; Tirado-Rives, J. *J. Am. Chem. Soc.* **1996**, *118*, 11225.
(24) Cornell, W. D.; Cieplak, P.; Bayly, C. I.; Gould, I. R.; Merz, K. M.; Ferguson, D. M.; Spellmeyer, D. C.; Fox, T.; Caldwell, J. W.; Kollman, P. A. *J. Am. Chem. Soc.* **1996**, *118*, 2309.

(25) MacKerell, A. D.; Bashford, D.; Bellott, M.; Dunbrack, R. L.; Evanseck, J. D.; Field, M. J.; Fischer, S.; Gao, J.; Guo, H.; Ha, S.; Joseph-McCarthy, D.; Kuchnir, L.; Kuczera, K.; Lau, F. T. K.; Mattos, C.; Michnick, S.; Ngo, T.; Nguyen, D. T.; Prodhom, B.; Reiher, W. E.; Roux, B.; Schlenkrich, M.; Smith, J. C.; Stote, R.; Straub, J.; Watanabe, M.; Wiorkiewicz-Kuczera, J.; Yin, D.; Karplus, M. *J. Phys. Chem. B* **1998**, *102*, 3586.

(26) Yan, T. Y.; Burnham, C. J.; Del Pópolo, M. G.; Voth, G. A. *J. Phys. Chem. B* **2004**, *108*, 11877.

(27) Breneman, C. M.; Wiberg, K. B. *J. Comput. Chem.* **1990**, *11*, 361.

(28) Williams, D. E.; Cox, S. R. *Acta Crystallogr. B* **1984**, *40*, 404.

(29) Williams, D. E.; Houpt, D. J. *Acta Crystallogr. B* **1986**, *42*, 286.

(30) Hsu, L. Y.; Williams, D. E. *Acta Crystallogr. A* **1980**, *36*, 277.

(31) Stone, A. J.; Alderton, M. *Mol. Phys.* **1985**, *56*, 1047.

(32) Bayly, C. I.; Cieplak, P.; Cornell, W. D.; Kollman, P. A. *J. Phys. Chem.* **1993**, *97*, 10269.

(33) Urahata, S. M.; Ribeiro, M. C. C. *J. Chem. Phys.* **2004**, *120*, 1855.

(34) Morrow, T. I.; Maginn, E. J. *J. Phys. Chem. B* **2002**, *106*, 12807.

(35) Canongia Lopes, J. N.; Deschamps, J.; Padua, A. A. H. *J. Phys. Chem. B* **2004**, *108*, 2038.

(36) Hanke, C. G.; Price, S. L.; Lynden-Bell, R. M. *Mol. Phys.* **2001**, *99*, 801.

(37) Liu, Z. P.; Huang, S. P.; Wang, W. C. *J. Phys. Chem. B* **2004**, *108*, 12978.

(38) Del Pópolo, M. G.; Lynden-Bell, R. M.; Kohanoff, J. *J. Phys. Chem. B* **2005**, *109*, 5895.

(39) Bühl, M.; Chaumont, A.; Schurhammer, R.; Wipff, G. *J. Phys. Chem. B* **2005**, *109*, 18591.

(40) Smith, W.; Leslie, M.; Forester, T. R. *DL_POLY*, v2.14; Daresbury Laboratories: Daresbury, Warrington, WA4 4AD, UK, 2003.

(41) Ercolessi, F.; Adams, J. B. *Europhys. Lett.* **1994**, *26*, 583.

(42) Lenosky, T. J.; Kress, J. D.; Kwon, I.; Voter, A. F.; Edwards, B.; Richards, D. F.; Yang, S.; Adams, J. B. *Phys. Rev. B* **1997**, *55*, 1528.

(43) Lenosky, T. J.; Sadigh, B.; Alonso, E.; Bulatov, V. V.; de la Rubia, T. D.; Kim, J.; Voter, A. F.; Kress, J. D. *Mod. Sim. Mater. Sci. Eng.* **2000**, *8*, 825.

(44) Umeno, Y.; Kitamura, T.; Date, K.; Hayashi, M.; Iwasaki, T. *Comput. Mater. Sci.* **2002**, *25*, 447.

(45) Li, Y. H.; Siegel, D. J.; Adams, J. B.; Liu, X. Y. *Phys. Rev. B* **2003**, *67*,

(46) Izvekov, S.; Voth, G. A. *J. Phys. Chem. B* **2005**, *109*, 6573.

(47) Marun, R. A. B.; Coronado, E. A.; Ferrero, J. C. *J. Comput. Chem.* **2005**, *26*, 523.

(48) Izvekov, S.; Parrinello, M.; Burnham, C. J.; Voth, G. A. *J. Chem. Phys.* **2004**, *120*, 10896.

(49) Kirkpatrick, S.; Gelatt, C. D.;Vecchi, M. P. *Science* **1983**, *220*, 671.

(50) Hansmann, U. H. E.; Okamoto, Y. *Curr. Opin. Struct. Biol.* **1999**, *9*, 177.

(51) Press, W. H.; Flannery, B. P.; Teukolsky, S. A.; Vetterling, W. T. *Numerical Recipes in Fortran 77*, 2nd ed.; Cambridge University Press: Cambridge, UK, 2001.

(52) Swamy, V.; Muscat, J.; Gale, J. D.; Harrison, N. M. *Surf. Sci.* **2002**, *504*, 115.

(53) Tosi, M. P.; Fumi, F. G. *J. Phys. Chem. Solids* **1964**, *25*, 45.

(54) Avent, A. G.; Chaloner, P. A.; Day, M. P.; Seddon, K. R.; Welton, T. *J. Chem. Soc., Dalton Trans.* **1994**, 3405.